Research article

Role of mitochondrial dysfunction in acute traumatic brain injury: Evidence from bioinformatics analysis

Fangfang Qian, Qi Zhong, Zhuoming Chen [*]

Department of Rehabilitation Medicine, The First Affiliated Hospital of Jinan University, Guangzhou, Guangdong, China

ARTICLE INFO

ABSTRACT

Background: The intricate regulatory relationship between mitochondrial dysfunction, apoptosis, and immune cells remains largely elusive following traumatic brain injury (TBI).
Methods: The GSE45997 dataset from the Gene Expression Omnibus database and utilized GEO2R to screen for differentially expressed genes (DEGs). Functional enrichment analyses were performed. Mitochondrial gene data from the MitoCarta3.0 database were combined with the DEGs to identify mitochondria-related DEGs (MitoDEGs). The hub MitoDEGs related to apoptosis were further screened. Animal models of TBI were established to investigate the mechanisms underlying mitochondrial dysfunction regulation of apoptosis. Furthermore, we explored the relationship between MitoDEGs/hub MitoDEGs and immune cells using the Spearman correlation method.
Results: Fifty-seven MitoDEGs were significantly enriched in pathways related to fatty acid degradation and metabolism. We identified three upregulated hub MitoDEGs, namely *Dnm1l*, *Mcl1* and *Casp3*, were associated with apoptosis. In the animal experiments, we observed significant expression levels of microtubule-associated protein 1 light chain 3 beta (LC3B) surrounding the injury site. Most LC3B-expressing cells exhibited positive staining for Beclin 1 and colocalization analysis revealed the simultaneous presence of Beclin 1 and caspase-3. The Western blot analysis further unveiled a significant upregulation of cleaved caspase-3 levels and LC3B II/LC3B I ratio after TBI. Moreover, the quantity of myeloid cell leukaemia-1 immunoreactive cells was notably higher than that in the control group. Spearman correlation analysis demonstrated strong associations between plasma cells, marginal zone B cells, native CD4 T cells, monocytes, and MitoDEGs/hub MitoDEGs.
Conclusions: This study sheds light on enhanced fatty acid metabolism following mitochondrial dysfunction and its potential association with apoptosis and immune cell activation, thereby providing new mechanistic insights into the acute phase of TBI.

1. Introduction

Traumatic brain injury (TBI) is the leading cause of death and disability, particularly among young individuals worldwide. In China, the prevalence of TBI surpasses that of most other nations, with an approximate population-based mortality rate of 13 cases per 100,000 people [1]. Furthermore, TBI survivors often encounter varying degrees of dysfunction, necessitating long-term medical care

---

* Corresponding author.
    E-mail address: zm120tchzm@qq.com (Z. Chen).

and rehabilitation, which places a substantial burden on both society and affected families. However, the underlying mechanisms driving TBI pathogenesis remain enigmatic, while effective treatment strategies remain elusive. In this context, it is imperative to enhance our understanding of TBI pathogenesis and explore potential therapeutic targets.

The brain, known for its elevated energy demands, is particularly vulnerable to mitochondrial dysfunction. Mitochondrial dysfunction, including calcium homeostasis imbalances, oxidative stress, disturbed energy metabolism, and mitophagy, has been identified in a variety of brain states and pathologies, including TBI. Apoptosis, a programmed cell death process predominantly executed through caspase 3 activation, is a major contributor to impaired neurological function in TBI patients. Notably, Feng et al. demonstrated a substantial reduction in apoptosis and infarct size through the inhibition of mitophagy in cerebral ischaemia–reperfusion injury [2]. Mitophagy initialization involves the activation of the evolutionarily conserved PTEN-induced putative kinase 1 (PINK1)/Parkin signalling pathway, which leads to enhanced phospho-ubiquitin conjugation on the outer mitochondrial membrane, facilitating the recruitment of microtubule-associated protein 1 light chain 3 (LC3) [3]. Additionally, Beclin 1, a crucial regulator, plays an important role in the initiation, autophagosome fusion, and proteolytic degradation of mitophagy [4]. It also plays a pivotal role in modulating the crosstalk between mitophagy and apoptosis by interacting with B-cell lymphoma (Bcl)-2 family proteins [5,6]. While recent studies indicate increased mitophagy following TBI [7,8], the precise role of mitophagy in TBI pathogenesis and neurological prognosis remains elusive.

Moreover, neuroinflammatory responses play an essential role in the early development of TBI, which appears to be driven primarily by overactivation of innate immune responses. The complement system has been identified as an important effector arm of the innate immune system that mediates excessive inflammatory responses after severe craniocerebral injury, leading to the breakdown of the blood–brain barrier, the development of brain oedema, and delayed induced cell death of neurons [9]. In animal models of midline fluid impaction, the levels of typical proinflammatory cytokines [such as interleukin (IL)-1β and tumour necrosis factor (TNF)-α] in the cortex peaked at 3–9 h [10]. Clinical studies have observed elevated levels of IL-6, IL-8, IL-10, TNF-α, and chemokine CC ligand-2 (CCL2) within the initial two days following TBI [11,12]. The elevation of these cytokines signifies immune cell activation and provides evidence for the correlation between activated immune responses and brain pathology. Activated immune cells have a high demand for energy. For example, in proinflammatory cells, such as activated monocytes and activated T and B cells, energy is produced by increased glycolysis, while in regulatory cells, such as regulatory T cells or M2 macrophages, energy is produced by increased mitochondrial function and beta-oxidation [13]. Therefore, mitochondria are potentially involved in the differentiation and activation processes of immune cells.

Currently, there is a lack of bioinformatics-based investigations focusing on the mechanism of mitochondrial dysfunction following TBI. Consequently, this study aims to bridge this knowledge gap by leveraging relevant microarray data from the Gene Expression Omnibus (GEO) database (GSE45997) [14] and conducting animal experiments. The primary hypothesis of this study posits that mitochondrial dysfunction plays a critical role in inducing apoptosis and contributes to the activation of immune cells during the acute phase of TBI.

2. Materials and methods

2.1. Microarray data

The TBI dataset was obtained from GEO (http://www.ncbi.nlm.nih.gov/geo). The search query involved utilizing the keyword "traumatic brain injury" and applying subsequent screening criteria for experiment type (expression profiling by array), animal species (Rattus norvegus), sample source (brain tissue), and modelling time. Ultimately, the dataset of interest, GSE45997, was selected for further analysis.

GSE45997 encompasses a total of three damaged hemispherical brain tissue samples obtained 24 h after TBI, along with three corresponding control samples.

2.2. Analysis of differentially expressed genes (DEGs)

Differential expression analysis was performed using GEO2R (https://www.ncbi.nlm.nih.gov/geo/geo2r/), an online analytical tool specifically designed for gene expression analysis. The DEGs of the two groups were filtered according to adjusted P value < 0.05 and $|\log2 \text{(Fold-change)}| \geq 1$.

To visualize the DEGs, a volcano plot and heatmap were generated. The volcano plot effectively represents the statistical significance of gene expression changes in relation to the fold change magnitude. The heatmap provides a visual representation of gene expression patterns and facilitates the identification of clustering and trends within the dataset. The generation of the volcano plot and heatmap was conducted using the bioinformatics platform (https://www.bioinformatics.com.cn/). This platform is widely recognized for its comprehensive suite of bioinformatics tools and resources and was utilized for the purpose of creating these visualizations.

2.3. Functional enrichment analysis

Gene Set Enrichment Analysis (GSEA) was employed to investigate not only differential genes but also more subtle pathway changes. Enrichment analysis of Kyoto Encyclopedia of Genes and Genomes (KEGG) pathways was utilized to identify the core pathways associated with the DEGs. Additionally, Gene Set Gene Ontology (GO) analysis was performed to assess gene functions across three categories: biological pathway (BP), cellular component (CC), and molecular function (MF). GSEA, KEGG, and GO enrichment

analyses were conducted using the bioinformatics platform. This platform is recognized for its comprehensive suite of bioinformatics tools and is well suited for conducting these enrichment analyses. To determine significant enrichment, the cut-off criterion was applied, specifying an adjusted P value < 0.05.

2.4. Analysis of mitochondria-related DEGs (MitoDEGs)

A total of 1140 mitochondrial localization genes were acquired from the mitochondrial protein database MitoCarta3.0 (http://www.broadinstitute.org/mitocarta). These genes were then intersected with the DEGs to identify MitoDEGs. To visualize the Mito-DEGs, a Venn diagram was generated using the online tool Venny2.1 (http://bioinformatics.psb.ugent.be/webtools/Venn/). This diagram effectively illustrates the shared and unique genes between the two datasets, providing insights into the overlap between mitochondrial localization genes and DEGs. Furthermore, a heatmap of the MitoDEGs was constructed using the bioinformatics platform. This heatmap visually represents the expression patterns of the MitoDEGs and allows for the identification of clustering and trends within the dataset.

2.5. Analysis of the protein–protein interaction (PPI) network and hub MitoDEGs

To investigate the protein–protein interaction network of the MitoDEGs, the online database STRING (https://string-db.org/) was employed. This database is widely recognized for its comprehensive collection of protein–protein interaction information. The resulting interactions were then visualized as a network using Cytoscape 3.8.2, a powerful software platform commonly used for network visualization and analysis.

To identify hub MitoDEGs, two plug-ins, namely, CytoHubba and MCODE, available within Cytoscape 3.8.2, were utilized. CytoHubba allows for the identification of highly connected genes within the network, while MCODE enables the detection of densely connected regions with higher functional significance. For MCODE, specific filter criteria were applied, including degree cut-off = 2; node score cut-off = 0.2; k-core = 2; and max depth = 100.

2.6. Analysis of hub MitoDEGs associated with apoptosis

The apoptosis gene set, consisting of 161 genes, was obtained from the GSEA database (https://www.gsea-msigdb.org/gsea/index.jsp). This gene set represents a collection of genes related to apoptosis. Subsequently, these genes were intersected with the DEGs to identify a subset referred to as apoptosis DEGs. This step aimed to identify genes involved in both apoptosis and differential expression.

To further refine the analysis, the overlapping genes between the apoptosis DEGs and hub MitoDEGs were selected. These represent DEGs that are involved in both apoptosis and mitochondrial localization and are potentially of high biological relevance.

By employing the online tool Venny2.1, the overlapping gene populations between the apoptosis gene set and DEGs were efficiently illustrated, thereby enhancing our understanding of the shared molecular components involved in apoptosis and DEGs. Moreover, to visualize the overlapping genes between the selected apoptosis DEGs and hub MitoDEGs, Venn diagrams were generated using Venny2.1. This tool facilitates the illustration of shared and unique genes between the two datasets, providing insights into the overlap between apoptosis DEGs and MitoDEGs.

2.7. TBI model and behavioral evaluation

Twenty-four male Sprague–Dawley rats, aged 8 weeks and weighing between 250 and 300 g, were procured from the Experimental Animal Center of Southern Medical University (license No. SCXK [Yue] 2021-0041). The rats were randomly divided into two groups: the control group and the TBI group, with twelve rats in each group. Following established protocols described in a previous study [15], the rat model of moderate TBI was induced using Feeney's weight-dropping method. Prior to the procedure, the rats were anaesthetized using pentobarbital. A circular bone piece with a diameter of 5 mm was precisely removed from the right hemisphere, with its centre located 1.5 mm posterior and 2.5 mm lateral to bregma. Subsequently, an impact force of 20 g × 30 cm was applied to the exposed area. In the control group, only the bone window was opened without applying any impact force. The behavior of the rats were evaluated using the modified neurological severity score (mNSS) [16], which includes assessments of motor function, sensory function, balance, and reflexes. This scoring system ranges from 1 to 18, with scores of 1–6 indicating mild neurological injury, scores of 7–12 indicating moderate neurological injury, and scores of 13–18 indicating severe neurological dysfunction. Two independent experimenters assessed the scores for each rat. Rats with mNSS scores falling within the range of 7–12 (indicating moderate injury) were chosen for further experimentation. Ethical approval for the animal study was granted by the Ethics Committee of the Nanfang Hospital of Guangzhou. All animal procedures were performed in strict accordance with the guidelines outlined in "The Guide for Care and Use of Laboratory Animals".

2.8. Immunofluorescence staining

At 24 h post-TBI, following anesthesia, six rats from each group received intracardiac injections of normal saline. Subsequently, the brain tissue was removed and fixed in 4 % paraformaldehyde. After dehydration with alcohol, paraffin sections were taken from the injured centre area in the TBI group and the corresponding brain area in the control group. One brain section of each rat was incubated overnight at 4 °C with anti-LC3B (rabbit, Abcam Cat# ab192890, RRID:AB_2827794), Beclin 1 (rabbit, Abcam, Cat# ab210498, RRID:

AB_2810879), caspase-3 (rabbit, Proteintech, Cat# 19677-1-AP, RRID:AB_10733244) and myeloid cell leukaemia-1 (Mcl1) (rabbit, Abcam, Cat# ab32087, RRID: AB_776245), followed by secondary antibodies for 3 h at room temperature. The sections were mounted with 4′,6-diamidino-2-phenylindole (DAPI) for nuclear staining to visualize and analyse the overall density of total cells. The regions of interest were defined as the cortical area immediately surrounding the injury site. Finally, fluorescence signals were examined under a confocal microscope.

2.9. Western blot assay

At 24 h post-TBI, six rats from each group were euthanized under anesthesia. The injured hemisphere was selected for Western blot analysis to assess the protein levels of LC3B and caspase-3. Tissue samples were homogenized in radio-immunoprecipitation assay lysis buffer, and the protein concentrations were determined using the bicinchoninic acid method. The proteins were separated by sodium dodecyl sulfate-polyacrylamide gel electrophoresis and transferred onto polyvinylidene fluoride membranes. Subsequently, the membranes were treated with a 5 % skimmed milk blocking solution at 37 °C for 1 h and then incubated overnight at 4 °C with primary antibodies against LC3B (rabbit, 1:10,000, Abcam Cat# ab192890, RRID:AB_2827794) and caspase-3 (rabbit, 1:1,000, Proteintech, Cat# 19677-1-AP, RRID:AB_10733244). After a series of washes with Tris buffered salineTween, the membranes were incubated with secondary antibody for 1 h at room temperature. Protein bands were visualized using a photo-chemiluminescence gel imaging system, and ImageJ software (National Institutes of Health, USA) was utilized for quantification analysis. Glyceraldehyde-3-phosphate de-hydrogenase (GAPDH) was used as an internal reference to calculate the relative expression of each antibody.

2.10. Analysis of the relationship between MitoDEGs/hub MitoDEGs and immune cells

The gene expression matrix was input into ImmuCellAI (http://bioinfo.life.hust.edu.cn/web/ImmuCellAI), which allowed us to estimate the infiltration abundance of 36 distinct immune cell types within each sample. To further investigate the potential relationships between MitoDEGs or hub MitoDEGs and immune cells, Spearman correlation analysis was performed. This statistical method enabled us to explore the associations between gene expression patterns and immune cell populations.

2.11. Statistical analysis

The measured data from the animal experiments are expressed as the mean ± standard deviation (SD). Statistical analysis was performed using SPSS 25.0 (IBM, Armonk, NY, USA). All data met the assumptions of normality. To assess the significance between two groups, Student's t-test was employed. Statistical significance was defined as a P value < 0.05.
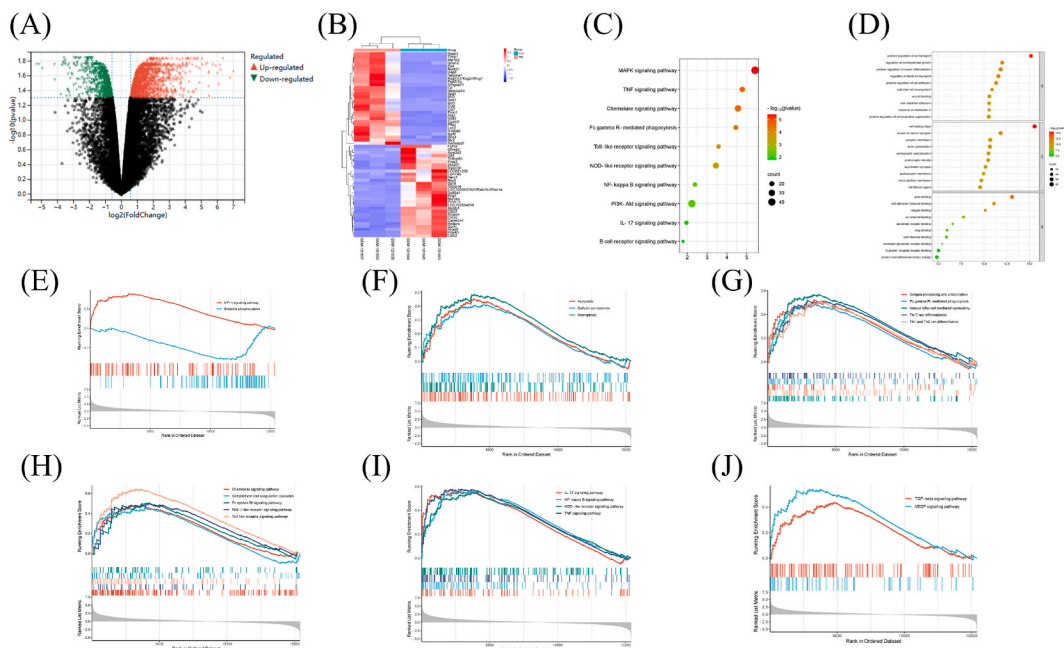

Fig. 1. The results of DEGs and functional enrichment analysis (A) Volcano plot of DEGs; (B) Clustered heatmap of DEGs; (C) KEGG pathway enrichment results of DEGs; (D) GO enrichment results of DEGs; (E) 2 significant GSEA sets in hypoxia; (F) 3 significant GSEA sets in cell death; (G, H) 10 significant GSEA sets in immunity; (I) 4 significant GSEA sets in inflammation; (J) 2 significant GSEA sets in growth factor.

3. Results

3.1. DEGs and functional enrichment analyses

The microarray expression profile dataset GSE45997 was downloaded from the GEO database. Difference analysis showed that compared with control samples, there were 1615 DEGs in the TBI samples, of which 1150 genes were upregulated and 465 genes were downregulated. The volcano plot and heatmap of the DEGs are shown in Fig. 1A and B.

The most enriched KEGG pathways among the DEGs were primarily associated with inflammation and immunity. These pathways include the MAPK signalling pathway, TNF signalling pathway, chemokine signalling pathway, and Fc gamma R-mediated phagocytosis, among others (Fig. 1C).

The DEGs were further categorized based on GO analysis, which revealed the most enriched BP, CC and MF. The enriched BP terms included ion transport, neuron differentiation, cell adhesion, and wound healing, among others. The CC terms highlighted neuronal synapse, synaptic membrane, actin cytoskeleton, and postsynaptic density, while the enriched MF terms emphasized actin binding, cell adhesion molecule binding, integrin binding, and others (Fig. 1D).

In addition, GSEA was performed to evaluate the functional significance of the genes in the TBI samples. The analysis unveiled the activation of several pathways associated with hypoxia, cellular death, immunity, and inflammation. These pathways include but are not limited to the HIF-1 signalling pathway, oxidative phosphorylation, apoptosis, necroptosis, cellular senescence, natural killer cell-mediated cytotoxicity, antigen processing and presentation, Fc gamma R-mediated phagocytosis, complement and coagulation cascades, IL-17 signalling pathway, NF-kappa B signalling pathway, TNF signalling pathway, and NOD-like receptor signalling pathway (Fig. 1E–I). Furthermore, pathways such as the VEGF signalling pathway and TGF-beta signalling pathway were also found to be enriched (Fig. 1J), indicating their potential involvement in TBI processes.

3.2. MitoDEGs, KEGG and GO pathway analyses

Mitochondria-related genes were extracted from the MitoCarta3.0 database, and genes that overlapped with DEGs were selected as MitoDEGs. We found 57 overlapping MitoDEGs, including 38 upregulated genes and 19 downregulated genes.
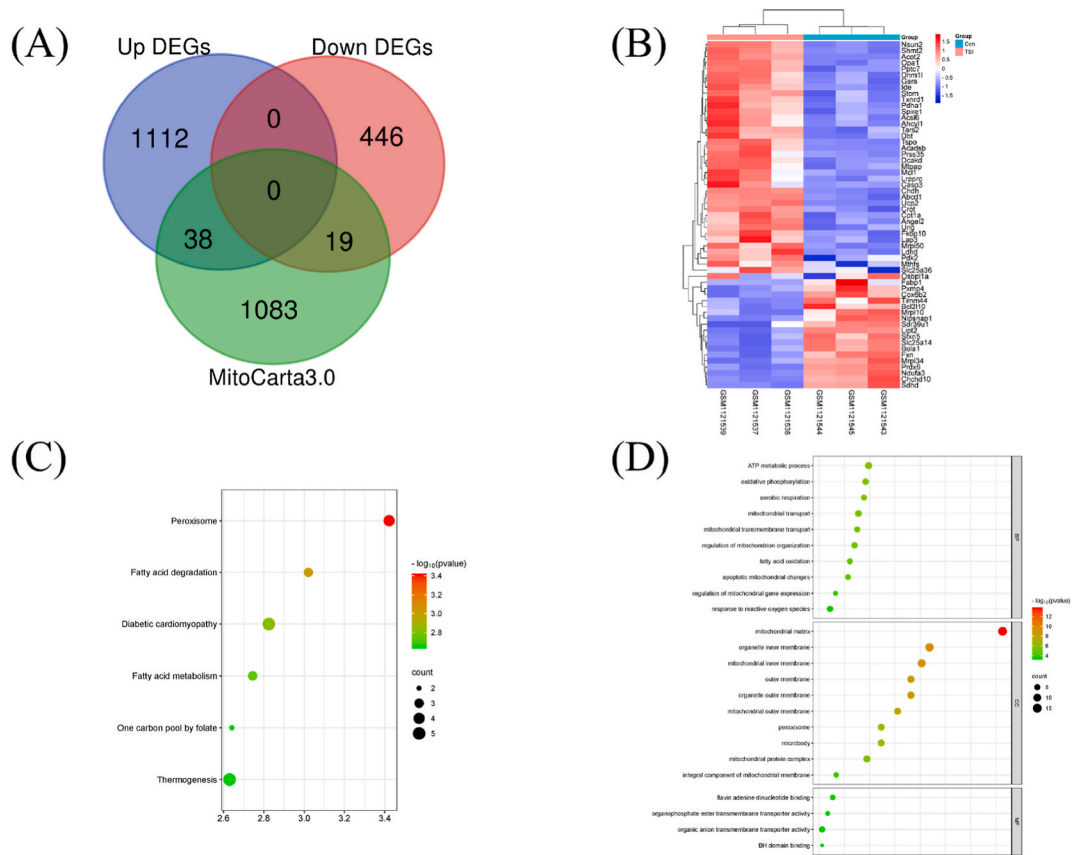

Fig. 2. The results of MitoDEGs, KEGG and GO pathway analyses (A) Venn diagram of MitoDEGs; (B) Clustered heatmap of MitoDEGs; (C) KEGG pathway enrichment results of MitoDEGs; (D) GO enrichment results of MitoDEGs.

The Venn diagram (Fig. 2A) visually represents the overlap between the mitochondria-related genes and the DEGs, highlighting the 57 genes that are involved. Additionally, a heatmap (Fig. 2B) offers a graphical depiction of the expression patterns of the MitoDEGs, enabling a comprehensive understanding of their transcriptional alterations.

To gain insights into the functional significance of the MitoDEGs, GO and KEGG enrichment analyses were performed. KEGG analysis revealed significant enrichment of the MitoDEGs in pathways associated with peroxisomes, fatty acid degradation, and fatty acid metabolism, among others (Fig. 2C). Furthermore, GO enrichment analysis revealed that the MitoDEGs were highly involved in oxidative phosphorylation, fatty acid oxidation, apoptotic mitochondrial changes, and various aspects of mitochondrial function and composition, among others (Fig. 2D).

3.3. PPI network of MitoDEGs and hub MitoDEGs

We obtained the PPI network from the STRING database, comprising 57 nodes and 46 edges. The network was visualized using Cytoscape, as depicted in Fig. 3A, providing a comprehensive overview of the interactions among the proteins. To identify key hub genes within the PPI network, we employed the MCC algorithm, a CytoHubba plug-in. As a result, 10 candidate hub genes were identified, namely, *Cpt1a, Dnm1l, Acadsb, Casp3, Shmt2, Dbt, Acot2, Tars2, Mcl1,* and *Acsl6* (Fig. 3B). Additionally, through the implementation of the MCODE plug-in, we discovered a significant module comprising 8 nodes and 22 edges within the PPI network. This module consists of several genes, including *Ucp2, Acadsb, Cpt1a, Acsl6, Mcl1, Fabp1, Casp3,* and *Dnm1l* (Fig. 3C). Finally, based on the analyses conducted, a total of 12 hub MitoDEGs were identified, including *Cpt1a, Dnm1l, Acadsb, Casp3, Shmt2, Dbt, Acot2, Tars2, Mcl1, Acsl6, Ucp2,* and *Fabp1*.

3.4. Hub MitoDEGs associated with apoptosis

The apoptosis gene set utilized in this study was sourced from the GSEA database, enabling the identification of 40 apoptosis DEGs through an intersection analysis with the DEGs. Then, the overlapping genes of apoptosis DEGs and hub MitoDEGs, including *Dnm1l, Mcl1,* and *Casp3,* were selected, which were upregulated after TBI (Fig. 3D and E).

3.5. Experimental validations of hub MitoDEGs associated with apoptosis

The mNSS scores of the control group rats were 0, and the mNSS scores of the TBI group rats were between 7 and 12, indicating that the TBI model was successfully established (Fig. 4A). In addition, there was no difference in body weight between the two groups of rats (Fig. 4B).

The results of nuclear staining showed that the total number of cells in the surrounding tissue increased significantly (F = 1.619, t = -12.793, dt = 10, p < 0.01) (Fig. 4C and D). Moreover, the immunoreactivity of LC3B surrounding the injury site was enhanced in the TBI group than in the control group (F = 1.979, t = -11.219, dt = 10, p < 0.01) (Fig. 4C and D). Nearly all LC3B-positive cells coexpressed Beclin 1, indicative of the prominent contribution of Beclin 1 to TBI-induced mitophagy (Fig. 4Ei). Noteworthily, a considerable proportion of Beclin 1-expressing cells displayed positive immunoreactivity for caspase-3, particularly when located in
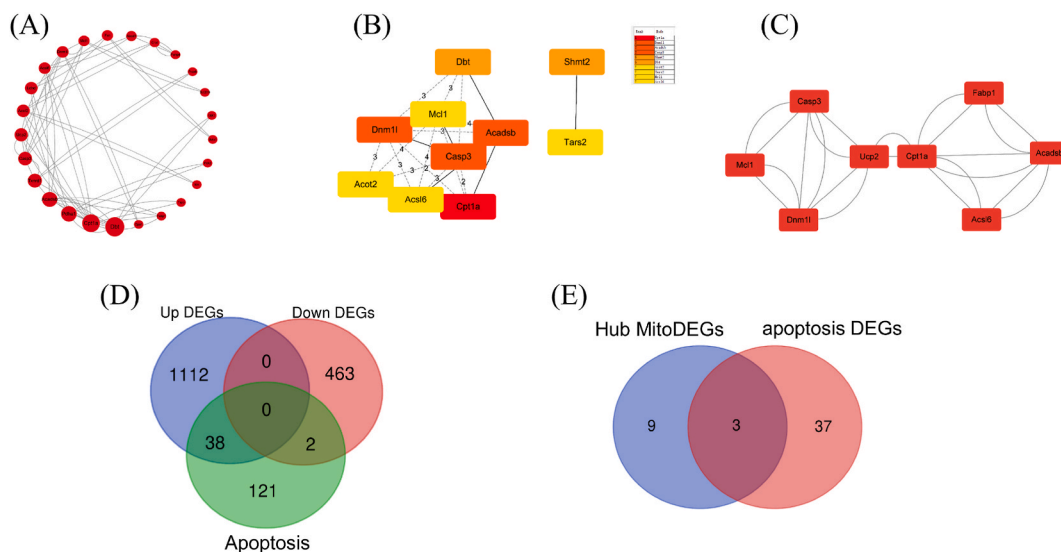

Fig. 3. The results of the PPI network of MitoDEGs and hub MitoDEGs (A) PPI network of MitoDEGs. (B) The top 10 hub genes were explored by CytoHubba. (C) A significant key cluster of 8 genes was identified as hub genes by MCODE; (D) Venn diagram of apoptosis DEGs; (E) Venn diagram of hub MitoDEGs associated with apoptosis.
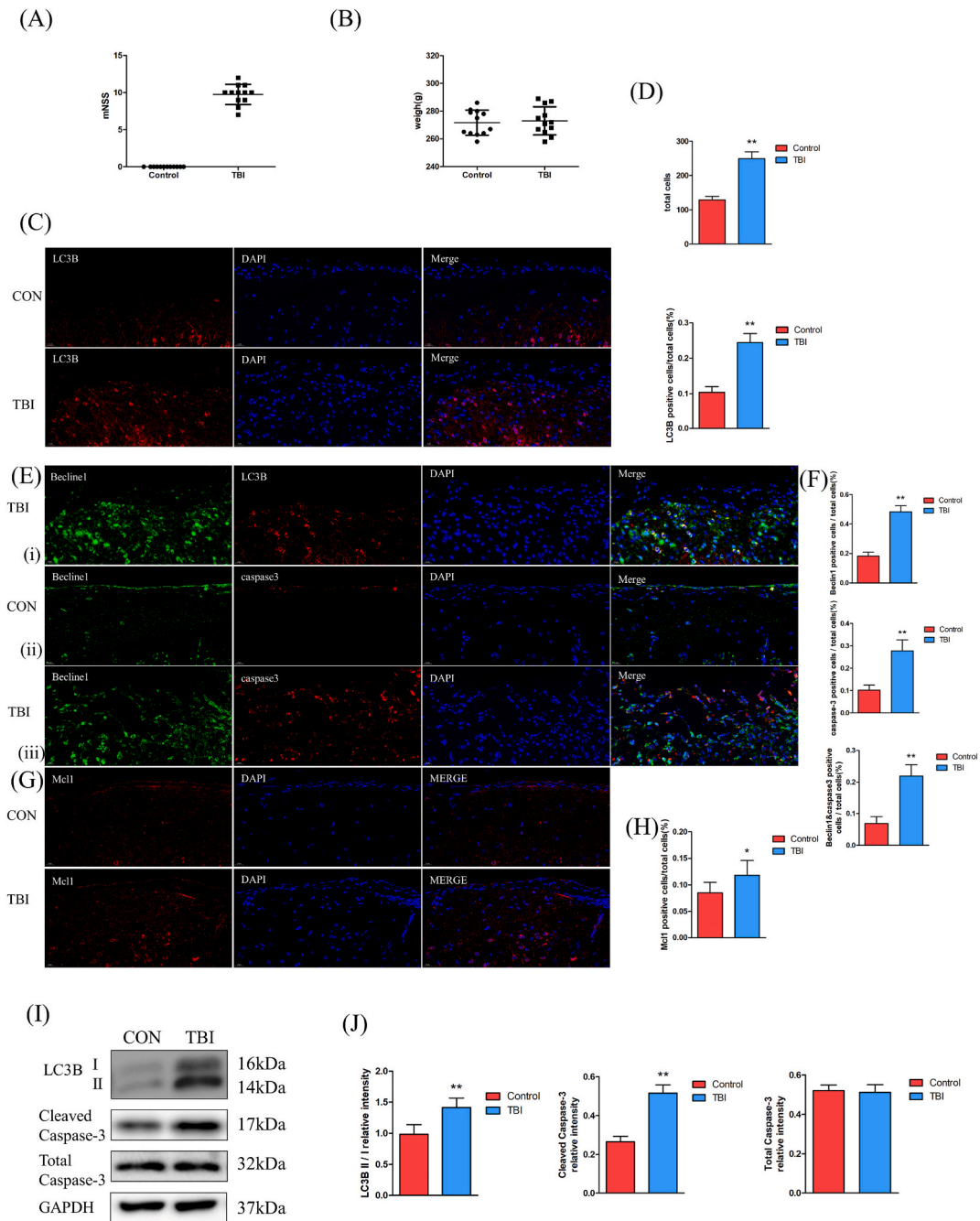
Fig. 4. The results of relationship between mitophagy and apoptosis at 24 h after TBI (A,B) mNSS and body weight of rats in the control and TBI groups. (C) Immunostaining showed the localization of LC3B in the control and TBI groups. (D) Quantification of total cells and LC3B + cells/total cells in the control and TBI groups. (E) Immunostaining showed the colocalization of Beclin 1 and LC3B in the TBI group (i) and the colocalization of Beclin 1 and caspase-3 in the control (ii) and TBI groups (iii). (F) Quantification of Beclin 1+ cells/total cells, caspase-3+ cells/total cells and Beclin 1+ & caspase-3+ cells/total cells in the control and TBI groups. (G) Immunostaining showed the localization of Mcl1 in the control and TBI groups. (H) Quantification of Mcl1+ cells/total cells in the control and TBI groups. (I) Western blot images representing protein levels of LC3B, cleaved caspase-3 and total caspase-3 in the injured hemisphere at 24h after TBI. (J) Bar graphs demonstrate semi-quantitations of LC3B II/LC3B I, cleaved caspase-3 and total caspase-3. Nuclei were stained blue with DAPI. 400 × magnification; scale bars: 20 μm. Data are shown as the mean ± SD (n = 6/group). *P < 0.05 and **P < 0.01 versus the control group. (For interpretation of the references to colour in this figure legend, the reader is referred to the Web version of this article.)

closer proximity to the centre of the injury (F = 3.771, t = −8.863, dt = 10, p < 0.01) (Fig. 4Eii-iii,F). These findings strongly suggest that upregulation of Beclin 1 partially contributes to the apoptotic process. The Western blot analysis further unveiled a significant upregulation of cleaved caspase-3 levels and LC3B II/LC3B I ratio subsequent to TBI (cleaved caspase-3: F = 1.358, t = −11.918, dt = 10, p < 0.01; LC3B II/LC3B I ratio: F = 0.025, t = −4.888, dt = 10, p < 0.01) (Fig. 4I and J). Furthermore, Mcl1-immunoreactive cells exhibited a statistically significant increase in the area surrounding the injury site compared to the control animals (F = 0.401, t = −2.389, dt = 10, p = 0.038) (Fig. 4G and H).

3.6. Relationship between MitoDEGs/hub MitoDEGs and immune cells

The relationship between MitoDEGs and immune cells is shown in Fig. 5A and B. It was found that plasma cells, marginal zone B cells, native CD4 T cells and monocytes were positively associated with 38 upregulated MitoDEGs and negatively associated with 19 downregulated MitoDEGs. Of the 12 hub MitoDEGs, *Fabp1* was negatively associated with native CD4 T cells; *Acot2* was positively associated with monocytes; *Dbt* and *Tars2* were positively associated with native CD4 T cells; *Cpt1a* was positively associated with plasma cells; *Casp3* was positively associated with marginal zone B cells; *Ucp2* was positively associated with native CD4 T cells and cDC2 cells; and *Mcl1* was negatively associated with M1 macrophages (Fig. 5C).

4. Discussion

The precise mechanism behind secondary injury following TBI remains unclear, and effective treatment strategies are currently lacking. Therefore, there is an urgent need to enhance our understanding of TBI pathogenesis and identify potential therapeutic targets. In this study, we utilized bioinformatics methods and animal experiments to investigate the pathogenesis of TBI. We initially observed that genes enriched in the oxidative phosphorylation pathway were significantly downregulated in damaged hemispheres compared to normal hemispheres. Conversely, genes enriched in the HIF-1, inflammation, and immune pathways demonstrated significant upregulation in the damaged hemispheres. These findings highlight the dysregulation of mitochondrial function in response to TBI and shed light on their potential role in the progression of secondary injury. Then, our study employed MitoCarta 3.0, a well-established mitochondrial proteome database, to identify 57 MitoDEGs. These genes were notably involved in pathways associated with fatty acid degradation and fatty acid metabolism. This suggests that mitochondrial metabolic disorders, particularly those related to fatty acid processes, play a critical role in TBI pathogenesis. Furthermore, mitochondrial dysfunction has been implicated in both apoptosis induction and immune cell activity. Thus, our study aims to analyse mitochondrial metabolic disorders and the regulatory role of mitochondrial dysfunction in apoptosis and immune dysregulation.

Apoptosis is widely recognized as a pivotal pathological characteristic of TBI. In our study, we identified three hub MitoDEGs, namely, *Dnm1l*, *Casp3*, and *Mcl1*, that were significantly upregulated and closely associated with apoptosis. Among these proteins, *Dnm1l* encodes dynamin-related protein 1 (Drp1), which plays a crucial role in mitochondrial recruitment and serves as a marker of mitophagy fission/fragmentation, suggesting that the increase in mitophagy may be related to apoptosis. This process is subsequently mediated by the PINK1/Parkin pathway, leading to the degradation of damaged mitochondria in most instances [17]. Impaired mitochondrial function results in an elevation of reactive oxygen species (ROS) levels, thereby causing cumulative damage to various cellular components, including proteins, genomes, and lipids. Theoretically, the selective elimination of dysfunctional mitochondria presents a critical protective mechanism that maintains cellular integrity. However, excessive self-digestion and degradation of vital intracellular components can ultimately culminate in cell death [18].

In our study, we conducted an animal experiment to provide evidence supporting the significant increase in mitophagy following TBI, which corresponded with the findings of a study by Lou et al. [19]. This phenomenon may be associated with the augmented accumulation of PINK1 kinase on the outer mitochondrial membranes due to decreased mitochondrial membrane potential (ΔΨm)
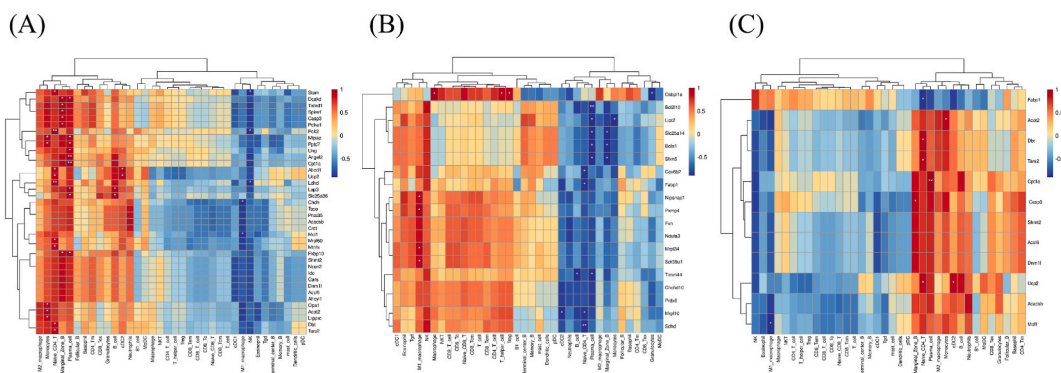

Fig. 5. The results of relationship between MitoDEGs/hub MitoDEGs and immune cells (A) The correlation between upregulated MitoDEGs and immune cells; (B) The correlation between downregulated MitoDEGs and immune cells; (C) The correlation betwee hub MitoDEGs and immune cells. Red represents a positive correlation, blue represents a negative correlation. *P < 0.05 and **P < 0.01. (For interpretation of the references to colour in this figure legend, the reader is referred to the Web version of this article.)

after hypoxia [20,21]. Studies have demonstrated that LC3 serves as a reliable marker for autophagosomes that represents mitophagy activity since the amount of LC3 has significant associations with the contents of autophagic vacuoles [22]. We observed a substantial increase in LC3B-positive cells in the vicinity of the injury site at 24 h post-TBI. Moreover, a majority of these LC3B-positive cells exhibited upregulation of Beclin 1, indicating a potential Beclin 1-dependent induction of mitophagy in TBI. Interestingly, we discovered that a significant portion of the Beclin 1-positive cells were also costained with caspase-3. Caspase-3 activation serves as a pivotal cumulative marker of cell death, as it plays a role in initiating both the intrinsic and extrinsic pathways of apoptosis. The activation of caspase-3 leads to the proteolysis of DNA repair proteins, cytoskeleton proteins, and the inhibitor of caspase-activated DNase, resulting in morphological changes and DNA damage. Furthermore, our investigation also revealed an increase in the number of Mcl1-positive cells. Mcl1, belonging to the anti-apoptotic Bcl-2 protein family, has been reported to interact with the BH3 domain in Beclin 1, consequently impeding excessive mitophagy and reducing apoptosis [23,24]. These findings suggest that Mcl1 may serve as a promising target for suppressing mitophagy in the context of TBI.

Following TBI, the excessive activation of N-methyl-D-aspartate receptor, α-amino-3-hydroxy-5-methyl-4-isoxazolepropionic acid receptor and various gated Na+ and Ca2+ channels results in elevated cytoplasmic Ca2+ and massive influx into mitochondria [25]. This heightened calcium activity not only results in diminished energy production but also stimulates the generation of ROS and reactive nitrogen species (RNS). Due to the presence of mitochondrial phospholipids rich in highly oxidizing polyunsaturated acyl chains, an optimal environment for lipid peroxidation (LP) is created [25]. Moreover, free fatty acids released by mitophagy can also boost LP. Under stress, lipid droplets accumulate near mitochondria and channel fatty acids to mitochondria [26,27]. Mitophagy wraps peridroplet mitochondria in autophagosomes that are subsequently degraded into free fatty acids and dispersed in the cytoplasm, and then oxidized to create lipid peroxides [28]. LP, a well-established contributor to post-TBI pathology, is a self-perpetuating process [29, 30]. The toxic aldehyde byproduct of LP, namely, 4-hydroxynonenal, progressively binds covalently to cellular and mitochondrial proteins, further compromising their function [31]. The mitochondrial and neuroprotective effects of various antioxidants have validated the role of LP in central nervous system secondary injury [32,33].

Furthermore, it is worth noting that mitochondria play a crucial role in regulating the differentiation and activation of immune cells. In our study, we identified several immune cell types that exhibited close associations with MitoDEGs, including monocytes, plasma cells, marginal zone B cells, and CD4 T cells. This implies that mitochondrial dysfunction may have implications beyond cellular survival and extend to immune cell functions. Previous research has demonstrated that brain injury results in a substantial increase in the absolute number of circulating monocytes [34]. The function of monocytes in response to TBI is comparable to that of microglia. Monocyte activation can be categorized into two distinct types: classical (bactericidal) activation and replacement (repair) activation. When monocytes are exposed to classical activators such as interferon-γ and CCL2, they generate an abundance of cytotoxic inflammatory mediators, including ROS and TNF [35]. In contrast, monocytes activated by interleukins (IL-4 and IL-13) express repair-related genes [35]. It has been observed that following TBI, the damaged cortex experiences a rapid increase in CCL2 (formerly known as monocyte chemoattractant protein-1, MCP-1) levels, impeding the repair of the lesion volume and negatively influencing neurological outcomes [36]. Additionally, Chen et al. reported that monocytes invade the brain parenchyma in response to brain trauma, exerting detrimental effects on neuronal survival and functional recovery [37]. B lymphocytes originate from progenitor cells residing in the bone marrow and subsequently enter the circulatory system, eventually migrating to the spleen and lymph nodes, where they form clusters. Upon encountering pathogens, B cells undergo activation and differentiate into plasma cells, which are primarily responsible for antibody production. Meissner et al. demonstrated that an elevation of the chemokine associated with B-cell chemotaxis, known as CCL20, occurred within 4 h after experimental brain injury (CCI) and persisted for 3 days [38]. Autoantibodies against central nervous system (CNS) proteins were present in the serum of patients with brain injury, suggesting that B cells initiated an immune response against brain-derived antigens after the injury [39]. Ankeny et al. proposed that activated B cells induce the pathological sequelae of spinal cord injury (SCI) by producing autoantibodies and activating the downstream inflammatory cascade, followed by microinjection of sera containing SCI antibodies into the intact CNS, causing hippocampal microglia/macrophage activation and prominent neuronal loss [40,41]. CD4 T cells have also been implicated in the induction of apoptosis in brain cells. They achieve this by either secreting inflammatory cytokines such as TNF-α or by utilizing FAS-dependent mechanisms [42].

In conclusion, the results of our investigation indicate that secondary damage occurs during the acute phase of TBI through several discernible mechanisms. First, an increase in mitophagy, a process involving the selective degradation of damaged mitochondria, has been observed, which could potentially lead to apoptosis. Additionally, there is evidence of enhanced fatty acid oxidation. Finally, it is noteworthy that mitochondrial dysfunction is closely associated with immune cell activation, implying an intricate interplay between these processes in TBI-induced secondary damage.

Data availability statement

Publicly available datasets were analysed in this study. These data can be found here: GEO database (https://www.ncbi.nlm.nih.gov/geo/), MitoCarta3.0 (http://www.broadinstitute.org/mitocarta) and GSEA database (https://www.gsea-msigdb.org/gsea/index.jsp).

CRediT authorship contribution statement

Fangfang Qian: Investigation, Methodology, Validation, Writing – original draft. **Qi Zhong:** Formal analysis, Writing – review & editing. **Zhuoming Chen:** Conceptualization, Project administration, Funding acquisition.

Declaration of competing interest

The authors declare that they have no known competing financial interests or personal relationships that could have appeared to influence the work reported in this paper.

References

[1] J.Y. Jiang, G.Y. Gao, J.F. Feng, Q. Mao, L.G. Chen, X.F. Yang, J.F. Liu, Y.H. Wang, B.H. Qiu, X.J. Huang, Traumatic brain injury in China, Lancet Neurol. 18 (2019) 286–295.
[2] J. Feng, X. Chen, B. Guan, C. Li, J. Qiu, J. Shen, Inhibition of peroxynitrite-induced mitophagy activation attenuates cerebral ischemia-reperfusion injury, Mol. Neurobiol. 55 (2018) 6369–6386.
[3] A.H. Rezaeian, W. Wei, H. Inuzuka, The regulation of neuronal autophagy and cell survival by MCL1 in Alzheimer's disease, Acta Mater Med 1 (2022) 42–55.
[4] Y. Sun, X. Yao, Q.J. Zhang, M. Zhu, Z.P. Liu, B. Ci, Y. Xie, D. Carlson, B.A. Rothermel, Y. Sun, B. Levine, J.A. Hill, S.E. Wolf, J.P. Minei, Q.S. Zang, Beclin-1-Dependent autophagy protects the heart during sepsis, Circulation 138 (2018) 2247–2262.
[5] R. Kang, H.J. Zeh, M.T. Lotze, D. Tang, The Beclin 1 network regulates autophagy and apoptosis, Cell Death Differ. 18 (2011) 571–580.
[6] H.D. Xu, Z.H. Qin, 1 Beclin, Bcl-2 and autophagy, Adv. Exp. Med. Biol. 1206 (2019) 109–126.
[7] Y. Luan, L. Jiang, Y. Luan, Y. Xie, Y. Yang, K.D. Ren, Mitophagy and traumatic brain injury: regulatory mechanisms and therapeutic potentials, Oxid. Med. Cell. Longev. 2023 (2023) 1649842.
[8] M. Zhu, X. Huang, H. Shan, M. Zhang, Mitophagy in traumatic brain injury: a new target for therapeutic intervention, Oxid. Med. Cell. Longev. 2022 (2022) 4906434.
[9] S. Weckbach, M. Neher, J.T. Losacco, A.L. Bolden, L. Kulik, M.A. Flierl, S.E. Bell, V.M. Holers, P.F. Stahel, Challenging the role of adaptive immunity in neurotrauma: rag1(-/-) mice lacking mature B and T cells do not show neuroprotection after closed head injury, J. Neurotrauma 29 (2012) 1233–1242.
[10] A.D. Bachstetter, R.K. Rowe, M. Kaneko, D. Goulding, J. Lifshitz, L.J. Van Eldik, The p38α MAPK regulates microglial responsiveness to diffuse traumatic brain injury, J. Neurosci. 33 (2013) 6143–6153.
[11] M.C. Morganti-Kossmann, P.M. Lenzlinger, V. Hans, P. Stahel, E. Csuka, E. Ammann, R. Stocker, O. Trentz, T. Kossmann, Production of cytokines following brain injury: beneficial and deleterious for the damaged tissue, Mol. Psychiatr. 2 (1997) 133–136.
[12] B.D. Semple, N. Bye, M. Rancan, J.M. Ziebell, M.C. Morganti-Kossmann, Role of CCL2 (MCP-1) in traumatic brain injury (TBI): evidence from severe TBI patients and CCL2-/- mice, J. Cerebr. Blood Flow Metab. 30 (2010) 769–782.
[13] M.M. Faas, P. de Vos, Mitochondrial function in immune cells in health and disease, Biochim. Biophys. Acta, Mol. Basis Dis. 1866 (2020) 165845.
[14] T.E. White, G.D. Ford, M.C. Surles-Zeigler, A.S. Gates, M.C. Laplaca, B.D. Ford, Gene expression patterns following unilateral traumatic brain injury reveals a local pro-inflammatory and remote anti-inflammatory response, BMC Genom. 14 (2013) 282.
[15] D.M. Feeney, M.G. Boyeson, R.T. Linn, H.M. Murray, W.G. Dail, I. Responses to cortical injury, Methodology and local effects of contusions in the rat, Brain Res. 211 (1981) 67–77.
[16] V. Sasso, E. Bisicchia, L. Latini, V. Ghiglieri, F. Cacace, V. Carola, M. Molinari, M.T. Viscomi, Repetitive transcranial magnetic stimulation reduces remote apoptotic cell death and inflammation after focal brain injury, J. Neuroinflammation 13 (2016) 150.
[17] G. Ashrafi, T.L. Schwarz, The pathways of mitophagy for quality control and clearance of mitochondria, Cell Death Differ. 20 (2013) 31–42.
[18] L. Shen, Q. Gan, Y. Yang, C. Reis, Z. Zhang, S. Xu, T. Zhang, C. Sun, Mitophagy in cerebral ischemia and ischemia/reperfusion injury, Front. Aging Neurosci. 13 (2021) 687246.
[19] C.L. Luo, B.X. Li, Q.Q. Li, X.P. Chen, Y.X. Sun, H.J. Bao, D.K. Dai, Y.W. Shen, H.F. Xu, H. Ni, L. Wan, Z.H. Qin, L.Y. Tao, Z.Q. Zhao, Autophagy is involved in traumatic brain injury-induced cell death and contributes to functional outcome deficits in mice, Neuroscience 184 (2011) 54–63.
[20] V. Jain, V. Choudhary, R. Pandit, Blood pressure target in acute brain injury, Indian J. Crit. Care Med. 23 (2019) S136–S139.
[21] S.M. Jin, M. Lazarou, C. Wang, L.A. Kane, D.P. Narendra, R.J. Youle, Mitochondrial membrane potential regulates PINK1 import and proteolytic destabilization by PARL, J. Cell Biol. 191 (2010) 933–942.
[22] I. Tanida, T. Ueno, E. Kominami, LC3 conjugation system in mammalian autophagy, Int. J. Biochem. Cell Biol. 36 (2004) 2503–2518.
[23] S. Pattingre, A. Tassa, X. Qu, R. Garuti, X.H. Liang, N. Mizushima, M. Packer, M.D. Schneider, B. Levine, Bcl-2 antiapoptotic proteins inhibit Beclin 1-dependent autophagy, Cell 122 (2005) 927–939.
[24] C. Xingyong, S. Xicui, S. Huanxing, O. Jingsong, H. Yi, Z. Xu, H. Ruxun, P. Zhong, Upregulation of myeloid cell leukemia-1 potentially modulates beclin-1-dependent autophagy in ischemic stroke in rats, BMC Neurosci. 14 (2013) 56.
[25] A.M. Lamade, T.S. Anthonymuthu, Z.E. Hier, Y. Gao, V.E. Kagan, H. Bayır, Mitochondrial damage & lipid signaling in traumatic brain injury, Exp. Neurol. 329 (2020) 113307.
[26] A. Herms, M. Bosch, B.J. Reddy, N.L. Schieber, A. Fajardo, C. Rupérez, A. Fernández-Vidal, C. Ferguson, C. Rentero, F. Tebar, C. Enrich, R.G. Parton, S.P. Gross, A. Pol, AMPK activation promotes lipid droplet dispersion on detyrosinated microtubules to increase mitochondrial fatty acid oxidation, Nat. Commun. 6 (2015) 7176.
[27] A.S. Rambold, S. Cohen, J. Lippincott-Schwartz, Fatty acid trafficking in starved cells: regulation by lipid droplet lipolysis, autophagy, and mitochondrial fusion dynamics, Dev. Cell 32 (2015) 678–692.
[28] P. Yang, J. Li, T. Zhang, Y. Ren, Q. Zhang, R. Liu, H. Li, J. Hua, W.A. Wang, J. Wang, H. Zhou, Ionizing radiation-induced mitophagy promotes ferroptosis by increasing intracellular free fatty acids, Cell Death Differ. 30 (2023) 2432–2445.
[29] R.L. Hill, J.R. Kulbe, I.N. Singh, J.A. Wang, E.D. Hall, Synaptic mitochondria are more susceptible to traumatic brain injury-induced oxidative damage and respiratory dysfunction than non-synaptic mitochondria, Neuroscience 386 (2018) 265–283.
[30] P. Zheng, N. Zhang, D. Ren, C. Yu, B. Zhao, Y. Zhang, Integrated spatial transcriptome and metabolism study reveals metabolic heterogeneity in human injured brain, Cell Reports Medicine 4 (2023) 101057.
[31] A.G. Mustafa, I.N. Singh, J. Wang, K.M. Carrico, E.D. Hall, Mitochondrial protection after traumatic brain injury by scavenging lipid peroxyl radicals, J. Neurochem. 114 (2010) 271–280.
[32] E.D. Hall, J.M. Braughler, P.A. Yonkers, S.L. Smith, K.L. Linseman, E.D. Means, H.M. Scherch, P.F. Von Voigtlander, R.A. Lahti, E.J. Jacobsen, U-78517F: a potent inhibitor of lipid peroxidation with activity in experimental brain injury and ischemia, J. Pharmacol. Exp. Therapeut. 258 (1991) 688–694.

[33] K. Wada, O.F. Alonso, R. Busto, J. Panetta, J.A. Clemens, M.D. Ginsberg, W.D. Dietrich, Early treatment with a novel inhibitor of lipid peroxidation (LY341122) improves histopathological outcome after moderate fluid percussion brain injury in rats, Neurosurgery 45 (1999) 601–608.

[34] S.G. Rhind, N.T. Crnko, A.J. Baker, L.J. Morrison, P.N. Shek, S. Scarpelini, S.B. Rizoli, Prehospital resuscitation with hypertonic saline-dextran modulates inflammatory, coagulation and endothelial activation marker profiles in severe traumatic brain injured patients, J. Neuroinflammation 7 (2010) 5.

[35] S. Gordon, F.O. Martinez, Alternative activation of macrophages: mechanism and functions, Immunity 32 (2010) 593–604.

[36] B.D. Semple, N. Bye, M. Rancan, J.M. Ziebell, M.C. Morganti-Kossmann, Role of CCL2 (MCP-1) in traumatic brain injury (TBI): evidence from severe TBI patients and CCL2-/- mice, J. Cerebr. Blood Flow Metabol. 30 (2010) 769–782.

[37] Y. Chen, J.M. Hallenbeck, C. Ruetzler, D. Bol, K. Thomas, N.E. Berman, S.N. Vogel, Overexpression of monocyte chemoattractant protein 1 in the brain exacerbates ischemic brain injury and is associated with recruitment of inflammatory cells, J. Cerebr. Blood Flow Metabol. 23 (2003) 748–755.

[38] C.L. Dalgard, J.T. Cole, W.S. Kean, J.J. Lucky, G. Sukumar, D.C. McMullen, H.B. Pollard, W.D. Watson, The cytokine temporal profile in rat cortex after controlled cortical impact, Front. Mol. Neurosci. 5 (2012) 6.

[39] A. Alam, E.P. Thelin, T. Tajsic, D.Z. Khan, A. Khellaf, R. Patani, A. Helmy, Cellular infiltration in traumatic brain injury, J. Neuroinflammation 17 (2020) 328.

[40] D.P. Ankeny, Z. Guan, P.G. Popovich, B cells produce pathogenic antibodies and impair recovery after spinal cord injury in mice, J. Clin. Invest. 119 (2009) 2990–2999.

[41] D.P. Ankeny, K.M. Lucin, V.M. Sanders, V.M. McGaughy, P.G. Popovich, Spinal cord injury triggers systemic autoimmunity: evidence for chronic B lymphocyte activation and lupus-like autoantibody synthesis, J. Neurochem. 99 (2006) 1073–1087.

[42] D. Fee, A. Crumbaugh, T. Jacques, B. Herdrich, D. Sewell, D. Auerbach, S. Piaskowski, M.N. Hart, M. Sandor, Z. Fabry, Activated/effector CD4+ T cells exacerbate acute damage in the central nervous system following traumatic injury, J. Neuroimmunol. 136 (2003) 54–66.